nature communications

Article

https://doi.org/10.1038/s41467-024-54388-7

The mortality impacts of greening Italy

Received: 9 November 2023

Accepted: 6 November 2024

Published online: 01 December 2024

Check for updates

Orazio Valerio Giannico[1,2,3], Rodolfo Sardone[1,2], Lucia Bisceglia[3], Francesco Addabbo[1,2], Francesco Pirotti[4,5], Sante Minerba[2] & Antonia Mincuzzi[1,2]

Green spaces have been shown to be beneficial to humans, but quantifying these benefits is a challenge for epidemiology. In this health impact assessment study, we exploit satellites to estimate for the whole of Italy the number of deaths that could be prevented in the 49 million adult population by greening residential areas. The exposure was assessed by calculating the normalized difference vegetation index at 10-m resolution within a 300-m distance from homes in 7904 municipalities. In this study we estimate, by achieving nationwide the level of residential greenness currently reached by the 25% of the population, a total of 28,433 (95% confidence interval: 21,400–42,350) preventable deaths and 279,324 (210,247–415,980) preventable years of life lost in Italy in 2022, representing the 5% of the total mortality burden. More green means fewer deaths, thus strong action is needed to increase the amount and accessibility of green spaces in all human settlements.

Green spaces, such as parks, playgrounds, and residential greenery, have been shown to have beneficial effects on people. They can promote mental and physical health and reduce morbidity and mortality among citizens[1–12]. The normalized difference vegetation index (NDVI) is a widely used satellite-derived metric that can quantify the vegetation in human settlements (e.g., street trees or general vegetation in public and private spaces)[11,13]. Several studies have highlighted the inverse relationship between NDVI and mortality[2–10]. Based on this evidence, a meta-analysis has estimated that the pooled relative risk (RR) for all-cause mortality per 0.1 increase in NDVI within a buffer of 500 m or less from a participant's home was 0.96 (95% CI 0.94–0.97)[11].

Several hypotheses have been considered to explain these findings. It has been proposed that physical activity is an important health determinant associated with green spaces. Green spaces can be places for recreational physical activity. In addition, green areas may encourage walking and cycling as forms of active transport[1,7,11,12,14,15]. However, a mediation analysis of one of the studies[4] included in the meta-analysis showed that physical activity accounted for 2.1% (95% CI 0.2;19.3%) of the association between green space and mortality[11]. Greenness can also have a number of beneficial health effects through ecosystem services, and has been shown to have a protective effect by reducing air pollution, noise, and the heat island effect[11,12,16–18]. Air pollution was included as a covariate in some of the studies[2,3,6] included in the meta-analysis, but the resulting RRs are not significantly different from those of studies that did not consider air pollution. After including air pollution in a mediation analysis, James and colleagues[4] found that $PM_{2.5}$ (fine particulate matter) could explain 4.4% (95% CI 2.4;7.7%) of the association between greenness and mortality, while Vienneu et colleagues[6] estimated a mediation of 2.4% (−0.2;5.5%) by PM_{10}[11].

Other proposed mechanisms to explain the health benefits of green spaces include stress reduction, enhanced relaxation, and restoration. One theory that explains the benefits of being in green spaces is the psychosomatic stress reduction theory. According to this idea, exposure to natural environments, such as views of them, could help people who are stressed out by putting them in a more positive emotional state[1,19,20]. In another study conducted in Dutch cities, the relationship between urban greenery and perceived general health was shown to be most strongly mediated by stress and social cohesion[21]. Finally, there is evidence linking green spaces to immunological function[22]. Li and colleagues[23,24] found an association between forest visits and enhanced immune responses, including the expression of

[1]Urban Health Center, House of Innovation for One Health, Taranto, Italy. [2]Unit of Statistics and Epidemiology, Local Health Authority of Taranto, Taranto, Italy. [3]Epidemiology and Care Intelligence Area, Regional Strategic Agency for Health and Social Care of Apulia, Bari, Italy. [4]Department of Land, Environment, Agriculture and Forestry, University of Padua, Padua, Italy. [5]Interdepartmental Research Center of Geomatics, University of Padua, Padua, Italy.
e-mail: oraziovaleriogiannico@gmail.com

anti-cancer proteins (such as granzymes A and B, granulysin, and perforin). It has also been suggested that exposure to a variety of microbes in their natural habitats may regulate immunity[25].

In terms of policy, the World Health Organization (WHO) suggests that a minimum of 0.5 hectares of green space should be available within a 300-m linear distance from homes[1]. The 3–30–300 rule for urban greening was proposed by urban forester Cecil Konijnendijk. It states that every home, school, and workplace should have at least three well-established trees in sight; every neighbourhood should have at least 30% tree cover; and every residence should be no more than 300 m from the nearest large public green space[26]. One way to link epidemiological evidence to public health policy is through health impact assessment (HIA), which combines meta-analytic effect measures with exposure and outcome data to estimate the health impacts under a counterfactual scenario[11,27–43].

Using the exposure-response function from Rojas-Rueda et colleagues[11], two large-scale health impact assessment studies were conducted in urban areas in the United States and in Europe to estimate the impacts of greenness on mortality[27,28]. According to the American HIA study[27], an increase of 0.1 NDVI units at the census tract level in the 35 most populous metropolitan areas could have prevented an estimated 38,187 deaths of people aged 65 and older in 2019. According to the European HIA study[28], which analysed 978 selected cities and 49 greater cities using 250-m resolution NDVI data, achieving a greenness level estimated to be in line with WHO recommendations[1] for access to green space could have reduced deaths by 42,968 in 2015.

However, the health benefits of exposure to greenness are likely to occur in all human settlements, not just selected cities or the more urbanised areas[4,7,11]. In addition, the use of different counterfactuals for each city (0.1 NDVI increase for all cities in the American study[27] and city-specific modelled targets in the European study[28]) may limit the comparability of the areas evaluated. Finally, there is uncertainty in the choice of target exposures due to the lack of specific recommendations for NDVI values[1,27,28].

Therefore, it may be worth exploring different methodological strategies and benefiting from updated and high-resolution data to assess the health impacts of greening interventions in all human settlements. To ensure comparability, it may be desirable to conduct these assessments using a single counterfactual exposure for all areas. Ideally, this NDVI target exposure should be as realistically achievable as possible, population-based, and possibly related to the existing green space recommendations. Finally, it would be desirable for this assessment to be replicable as far as possible around the world, using available software and data.

In the present study we want to meet all these needs by capitalising on satellite-derived residential exposure data at 10-m resolution for the whole of Italy in 2022. The aim of this health impact assessment is to estimate the total adult mortality burden that could be prevented in all Italian municipalities by greening residential areas up to the level of greenness currently achieved by the 25% of the population.

Results

Population and exposure

The total adult population (≥20 years) in all 7,904 Italian municipalities in 2022 is 48,628,328. All exposures to greenest period NDVI (2022) and to specific land cover classes (2021) at 10 m resolution were calculated within 300 m of homes (population-buffers). Maps of greenest period NDVI, population-weighted exposure (PWE) to greenest period NDVI, and population counts are shown in Figs. 1 and 2 and Supplementary Fig. 1, respectively. Population-weighted percentiles of exposures to greenest period NDVI, exposures to land cover classes, and adult population counts are reported in Supplementary Table 1. The 25th, 50th, 75th and 95th population-weighted percentiles of PWEs to greenest period NDVI in all the Italian municipalities are 0.30, 0.36, 0.43 and 0.54, respectively. The 25th, 50th, 75th and 95th population-weighted percentiles of greenest period NDVI in all the Italian 300 m population buffers are 0.27, 0.36, 0.46 and 0.60, respectively. The unweighted percentiles of these measures and the weighted percentiles of these measures when excluding sparsely populated areas in the exposure assessment are reported in Supplementary Tables 2 and 3, respectively.

The counterfactual exposure of the health impact assessment was set at 0.46, which is the 75th population-weighted percentile of the greenest period NDVI in all the 300-m radius population-buffers. This is the target level of greenness which is currently achieved by the 25% of the Italian population. In the study area, a PWE to greenest period NDVI of 0.46 within 300 m from the residence approximately corresponds to a PWE to tree cover proportion of 30% within the same distance.

Health impact assessment

The results of the HIA are reported in Tables 1–3 and in Supplementary Figs. 2 and 3 for all the 39,803,860 adult inhabitants of the 3720 Italian municipalities that have a PWE to greenest period NDVI below the counterfactual exposure of 0.46 in 2022. Considering the whole of Italy, the PWEs to tree cover proportion, green area proportion and greenest period NDVI are 21.2%, 32.3% and 0.33, respectively.

A total of 28,433 (95% CI 21,400–42,350) annual preventable deaths, 71 (95% CI 54–106) annual preventable death rate (per 100,000 inhabitants) and 5.0% (95% CI 3.7–7.4%) annual preventable death rate fraction were estimated for Italy in 2022. The estimated number of preventable deaths per year is 12,377 (95% CI 9,317–18,428) in provincial capitals and 16,056 (95% CI 12,083–23,923) in non provincial capitals. The higher preventable death rate was estimated for provincial capitals (86 deaths per 100,000) and for provincial capitals with a population of 120,000 or more (93 deaths per 100,000). The higher preventable death rate fraction was estimated for provincial capitals (5.8% of deaths) and for provincial capitals with a population of 120,000 or more (6.3% of deaths). Considering all municipalities, the higher preventable death rate was estimated for the population aged ≥80 years (504 deaths per 100,000) and the higher preventable death rate fraction for the population aged <80 years (5.1–5.2% of deaths).

A total of 279,324 (95% CI 210,247–415,980) annual preventable years of life lost (YLL), 702 (95% CI 528–1,045) annual preventable YLL rate (per 100,000 inhabitants) and 5.0% (95% CI 3.8–7.5%) annual preventable YLL rate fraction were estimated for Italy in 2022. The estimated number of preventable YLL per year is 118,257 (95% CI 89,030–176,040) in provincial capitals and 161,066 (95% CI 121,217–239,940) in non provincial capitals. The higher preventable YLL rate was estimated for provincial capitals (826 YLL per 100,000) and for provincial capitals with a population of 120,000 or more (893 YLL per 100,000). The higher preventable YLL rate fraction was estimated for provincial capitals (5.9% of YLL) and for provincial capitals with a population of 120,000 or more (6.4% of YLL). Considering all municipalities, the higher preventable YLL rate was estimated for the population aged ≥80 years (2575 YLL per 100,000) and the higher preventable YLL rate fraction for the population aged <80 years (5.1–5.2% of YLL).

The findings of the uncertainty and sensitivity analyses for the HIA are reported in the Supplementary Notes 1–2 and in Supplementary Table 4. There were no relevant changes from using a different greenest period or satellite, excluding sparsely populated areas, applying a 20% reduction of the effect in non provincial capitals, or using an alternative approach to calculating the preventable fractions. Lower estimates were obtained by using as counterfactual exposures the 75th population-weighted percentile of the municipality-level PWEs to greenest period NDVI or the 50th population-weighted percentiles. Higher estimates were obtained by using as counterfactual exposures the 75th unweighted percentiles or the 95th population-weighted percentiles, or by using other exposure-response functions.

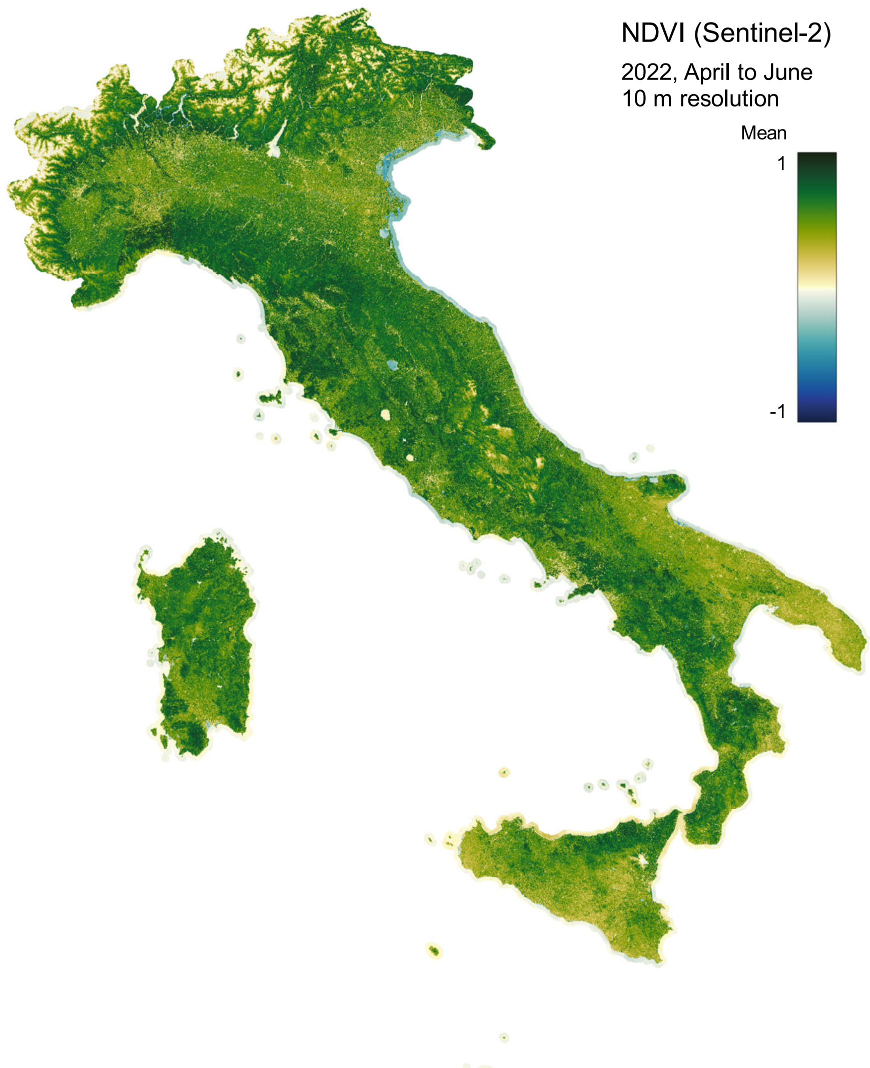

Fig. 1 | Greenest period NDVI from Sentinel-2. Mean per pixel. Italy with a 5 km buffer around the boundaries, including water bodies, April-June 2022. World Mollweide (ESRI:54009). NDVI: normalized difference vegetation index. Map created with QGIS version 3.28.4. NDVI data from Sentinel-2 are available at: https://code.earthengine.google.com (European Union. Copernicus Programme. Sentinel-2 mission. Image collection: 'COPERNICUS/S2_SR_HARMONIZED').

Analysis of land cover

The results of Spearman correlations and generalised additive mixed effect models (GAMM) between the PWEs to relative land cover measures and the PWE to greenest period NDVI are shown in Table 4 (Spearman correlation, single-predictor models and multiple-predictor models), Fig. 3 (single-predictor models) and Fig. 4 (multiple-predictor models). The plots are helpful in observing the estimated functional forms, while the statistics reported in the table identify the most influential measures.

The proportion measures most influential in determining the PWE to greenest period NDVI appear to be the built-up (ρ −0.87; adjusted R^2 0.93; null deviance explained 0.94), the green area (ρ 0.86; adjusted R^2 0.91; null deviance explained 0.93) and the tree cover (ρ 0.77; adjusted R^2 0.82; null deviance explained 0.84). The model with both tree cover and grassland proportion shows similar results (adjusted R^2 0.92; null deviance explained 0.93). The ratio-to-built-up (odds) measures most influential in determining the PWE to greenest period NDVI appear to be the green area (ρ 0.89; adjusted R^2 0.94; null deviance explained 0.95) and the tree cover (ρ 0.87; adjusted R^2 0.89; null deviance explained 0.91). The model with both tree cover and grassland ratio-to-built-up shows similar results (adjusted R^2 0.93; null deviance explained 0.94). The estimated functional forms of these relationships are shown in Figs. 3 and 4. The shaded areas show confidence bands at 2 standard errors above and below the estimates. Rug plots show the distribution of the data. Especially in the spaces with denser data distributions and narrower confidence intervals, the greenest period NDVI increases with increasing tree cover and green area.

Applying various sensitivity analyses to the GAMMs did not lead to any significant changes in the results. The estimates from excluding sparsely populated areas, or from changing the smoothing terms are similar to the estimates from the main analysis. We have reported the results from the models without random effects and/or population weights in Supplementary Tables 5–7 and in Supplementary Figs. 4–9. As in the main analysis, in the spaces with denser data distributions and narrower confidence intervals, the greenest period NDVI increases with increasing tree cover and green area.

Discussion

In this a nationwide health impact assessment study, we estimate the number of deaths that could be prevented in Italy by greening residential areas up to the level of greenness currently achieved by the 25% of the population. Exposure was assessed within a 300-m distance from homes capitalising on satellite images at 10-m resolution. The estimated total mortality burden in the 49 million adult population

https://doi.org/10.1038/s41467-024-54388-7

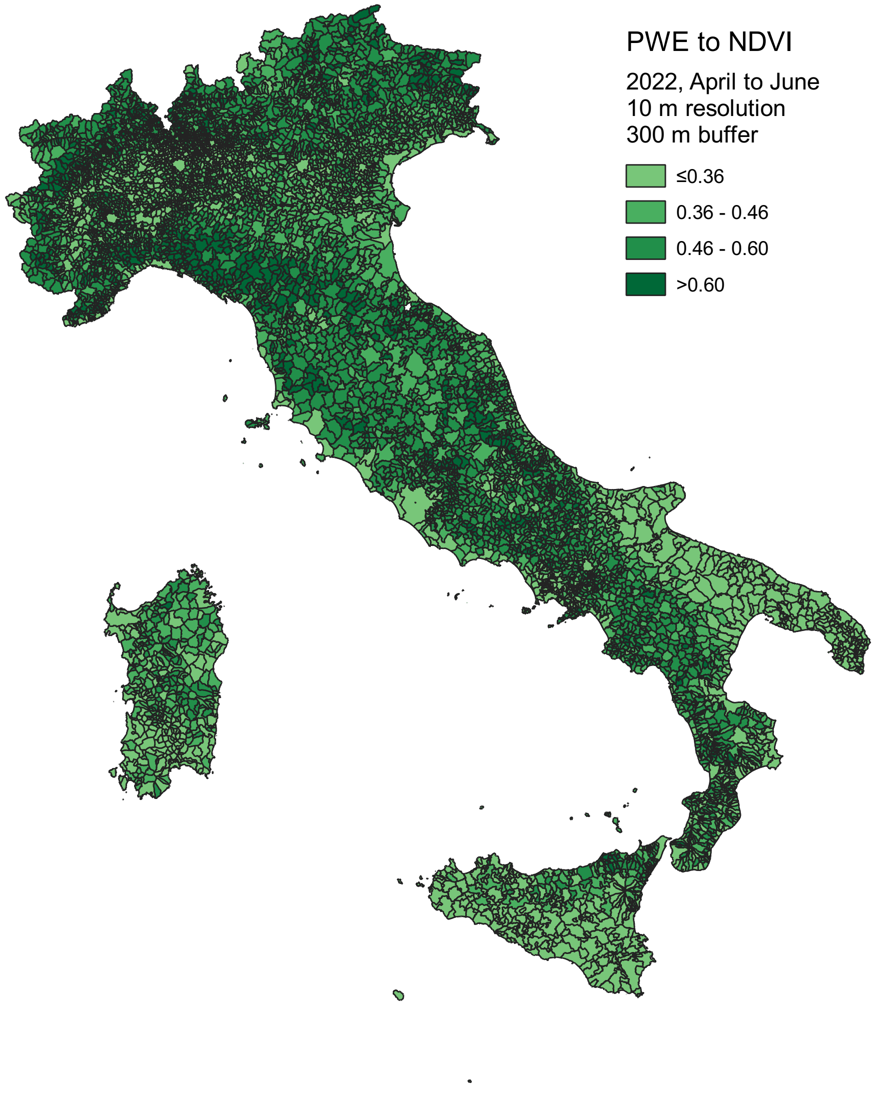

Fig. 2 | Greenest period NDVI from Sentinel-2. PWE per municipality. Italy, April-June 2022. WGS 84 / UTM zone 32N (EPSG:32632). NDVI: normalized difference vegetation index. PWE: population-weighted exposure. Map created with QGIS version 3.28.4. Population data from GHSL are available at: https://ghsl.jrc.ec.europa.eu/download.php?ds=pop (Global Human Settlement Layer. GHS population grid (R2023). Product: GHS-POP, epoch: 2020, resolution: 100 m, coordinate system: Mollweide). NDVI data available are at: https://code.earthengine.google.com (European Union. Copernicus Programme. Sentinel-2 mission. Image collection: 'COPERNICUS/S2_SR_HARMONIZED').

varies from 2.1% in the less populated not provincial capitals to 6.3% in the more populated provincial capitals. This findings are also consistent with the estimated proportions of tree cover and green area for each group of municipalities. Evaluation of less ambitious NDVI targets resulted in lower but still relevant mortality estimates.

Green space exposure depends not only on the amount of green space, but also on its spatial distribution in relation to the population. Areas that are green but far from homes do not contribute to the residential exposure. Unlike previous HIA studies[27,28,43] which set different targets for each city, we experimented with using a single population-based target level of greenest period NDVI to ensure comparability of estimates. In addition, Barboza et colleagues[28] stated that a greater number of deaths could be prevented by providing more green space than recommended by the WHO[1].

Our main exposure target of 0.46 was based on measured data, namely the 75th population-weighted percentile of the greenest period NDVI calculated for the whole country within 300-m distance of homes. This approach is consistent with the WHO and Konijnendijk recommendations for the 300-m distance[1,26]. Furthermore, in the study area, a PWE to greenest period NDVI of 0.46 within 300 m from residence approximately corresponds to a PWE to tree cover proportion of 30% within the same distance. The only element of the 3–30–300 rule that we could not directly assess on a large scale was the presence of three trees visible from the house, which would require data with a higher spatial resolution. We also couldn't assess the quality or actual accessibility of the green space within the 300-m distance. Taking these limitations into account, the population-based counterfactual target of 0.46 on average seems to correspond roughly to the 30–300 part of the 3–30–300 rule in Italy. In the future, it would be interesting to assess the population-weighted NDVI exposure in specific Italian areas or in other countries, and how local NDVI measures relate to the land cover measures and to the Konijnendijk's rule.

The analysis of land cover data in the present study suggests the essential role of trees in residential areas in Italy, followed by grassland. The ratio-to-built-up measures are more strongly associated with the greenest period NDVI, and the ratio-to-built-up of green area and tree cover explain much of the variability in NDVI. In Italy, on average, the single most influential positive NDVI determinant appears to be the

Table 1 | Population and exposure to greenness in the municipalities included in the HIA when using as counterfactual exposure (*k*) the 75th population-weighted percentile of greenest period NDVI in all the 300 m population-buffers. Italy, 2021 (land cover) and 2022 (NDVI and population)

N = 3720 municipalities with a PWE to greenest period NDVI < 75th percentile (*k* = 0.46)	Population	Exposure to greenness			
	Number	PWE			
	≥20 years	Three cover proportion [%]	Green area proportion [%]	Greenest period NDVI	Difference between *k* and the greenest period NDVI
Italy (*n* = 3720)	39,803,860	21.2	32.3	0.33	0.13
Provincial capitals (*n* = 105)	14,315,146	22.5	29.1	0.31	0.15
<45,000 inhabitants (*n* = 27)	900,421	28.5	38.3	0.38	0.08
45–75,000 inhabitants (*n* = 25)	1,425,795	24.3	33.8	0.33	0.13
75–120,000 inhabitants (*n* = 26)	2,356,217	20.6	29.7	0.33	0.13
≥120,000 inhabitants (*n* = 27)	9,632,713	22.1	27.5	0.30	0.16
Non provincial capitals (*n* = 3615)	25,488,714	20.5	34.1	0.35	0.11
<1000 inhabitants (*n* = 454)	286,150	25.6	45.0	0.41	0.05
1–2000 inhabitants (*n* = 592)	869,361	24.4	42.9	0.40	0.06
2–5000 inhabitants (*n* = 1049)	3,469,672	22.0	39.4	0.38	0.08
≥5000 inhabitants (*n* = 1520)	20,863,531	20.0	32.7	0.34	0.12

Population data from GHSL are available at: https://ghsl.jrc.ec.europa.eu/download.php?ds=pop (Global Human Settlement Layer. GHS population grid (R2023). Product: GHS-POP, epoch: 2020, resolution: 100 m, coordinate system: Mollweide). NDVI data from Sentinel-2 are available at: https://code.earthengine.google.com (European Union. Copernicus Programme. Sentinel-2 mission. Image collection: 'COPERNICUS/S2_SR_HARMONIZED'). Land cover data from WorldCover are available at: https://code.earthengine.google.com (European Space Agency. WorldCover Project. 2021. Image collection: 'ESA/WorldCover/v200').

HIA health impact assessment, *NDVI* normalized difference vegetation index, *PWE* population-weighted exposure.

tree cover, while the most influential negative NDVI determinant appears to be the human built environment. Thus, the ratio-to-built-up measures seem to be more specific indicators of human exposure to green spaces than the proportion measures. Therefore, it is of utmost importance to integrate urban green spaces into urban centres. This will disassociate the built environment from the absence of greenness and is likely to reduce mortality.

These findings are consistent with published research on the beneficial effects of trees on human health[12,44–56]. In general, trees have been associated with reducing harms (excessive heat, air pollution, noise, ultraviolet radiation, crime), restoring capacities (effects on cognition and attention, mental health, mood, anxiety, psychophysiological stress and clinical outcomes), and building capacities (impacts on birth outcomes, immune system, active living, weight status, cardiovascular function, social cohesion)[12,44,45]. Urban trees have been shown to have specific benefits in the areas of health and social well-being (they reduce pollution, improve physical and mental health, strengthen community bonds, increase physical activity, decrease aggression and violence, reduce crime), cognitive development and education (they improve student performance, reduce stress, increase concentration, improve attention and self-discipline), economy and resources (high return-on-investment, support tourism, increase houses prices and rents, reduce energy use and bills, promote food sustainability, provide resources and firewood), climate change mitigation and habitat (they reduce the urban heat island effect, store and sequester carbon, provide critical habitat), and green infrastructure (they manage stormwater and protect aquatic and terrestrial life)[12,45,46].

Natural capital is the term used to describe components of the environment that provide value to people, either directly or indirectly. Many countries are currently in the process of identifying the location, quality, and ecosystem services that make up their natural capital assets and contribute to human well-being, not only in rural areas but also in urban areas. Urban trees are an example of this type of natural capital[47]. When Kardan and colleagues used high-quality public health and demographic data to compare neighbourhoods in Toronto with different densities of street trees, they found a correlation between higher tree density and lower incidence of heart and metabolic disease, as well as better health perceptions. According to the authors, planting just ten or more trees per city block can save a household from paying over $10,000 in medical costs. This amount far exceeds the projected costs of planting and maintaining those for ten additional trees[48]. Similarly, Beyer et al. examined a range of urban and rural settings in Wisconsin, USA, and found that having more trees in a neighbourhood − measured as a higher percentage of tree canopy − was associated with better mental health, especially for people aged 55 and older, after adjusting for a wide range of confounders[49].

Similarly, in a cross-sectional study conducted in London, UK, Taylor and colleagues found that street tree density was lower in areas where smoking and antidepressant prescription rates were higher. Prescriptions for antidepressants were correlated with smoking levels, but the relationship between the number of trees and depression prescriptions persisted even after confounding variables were taken into account[50]. Strong evidence for the benefits of trees to human health can also be found in Donovan and colleagues' analysis of the consequences of city tree removal. The study analysed health data before and after the emerald ash borer infestation that resulted in the loss of 100 million ash trees in 1296 U.S. counties between 1990 and 2007. They discovered that the loss of trees was linked to statistically significant increases in mortality from lower respiratory tract and cardiovascular diseases[51]. More neighbourhood tree cover was linked to better overall health, independent of access to green space, according to a study by Ulmer and colleagues using LIDAR (Light Detection and Ranging) data in California. This association was primarily mediated by lower overweight/obesity and better social cohesion, and to a lesser extent by lower type 2 diabetes, high blood pressure, and asthma. According to these results, nature and trees have a significant impact on improving overall population health in urban environments[52].

According to Astell-Burt and Feng, people with ≥30% tree cover have a decreased risk of heart disease, hypertension, and diabetes than those with 0–9% tree canopy. In addition, research revealed that areas with ≥30% tree canopy has decreased prevalence of diabetes, hypertension, and heart disease than areas with 0–9% tree cover[53]. Schwaab et al. show that urban trees in most European cities have lower temperatures than the urban fabric during summer and heat waves. When compared to continuous urban fabric, land surface temperatures recorded for urban trees are, on average, 0–4 K lower in Southern

https://doi.org/10.1038/s41467-024-54388-7

Table 2 | Estimated preventable deaths in the municipalities included in the HIA when using as counterfactual exposure (*k*) the 75th population-weighted percentile of greenest period NDVI in all the 300 m population-buffers. Italy, 2022

N = 3720 municipalities with a PWE to greenest period NDVI < 75th percentile (*k* = 0.46)	Preventable deaths														
	Number (95% CI)					Rate (95% CI) [per 100,000 inhabitants]					Rate fraction (95% CI) [%]				
	20–39 years	40–59 years	60–79 years	≥80 years	≥20 years	20–39 years	40–59 years	60–79 years	≥80 years	≥20 years	20–39 years	40–59 years	60–79 years	≥80 years	≥20 years
Italy (*n* = 3720)	216 (162–321)	1671 (1258–2487)	8148 (6133–12,131)	18,400 (13,847–27,411)	28,433 (21,400–42,350)	2 (2–3)	11 (9–17)	73 (55–108)	504 (379–750)	71 (54–106)	5.2 (3.9–7.8)	5.2 (3.9–7.7)	5.1 (3.9–7.6)	4.9 (3.7–7.3)	5.0 (3.7–7.4)
Provincial capitals (*n* = 105)	84 (63–125)	671 (505–999)	3413 (2569–5079)	8210 (6179–12,226)	12,377 (9317–18,428)	2 (2–3)	13 (10–19)	85 (64–126)	572 (430–851)	86 (65–129)	6.0 (4.5–8.9)	6.0 (4.5–8.9)	6.0 (4.5–8.9)	5.7 (4.3–8.5)	5.8 (4.4–8.6)
<45,000 inhabitants (*n* = 27)	3 (3–5)	24 (18–37)	128 (96–191)	333 (250–499)	488 (366–732)	2 (1–2)	8 (6–12)	47 (35–71)	348 (261–521)	54 (41–81)	3.5 (2.6–5.2)	3.4 (2.6–5.1)	3.4 (2.5–5.1)	3.3 (2.5–5.0)	3.3 (2.5–5.0)
45–75,000 inhabitants (*n* = 25)	8 (6–12)	59 (45–88)	309 (233–460)	714 (538–1063)	1091 (821–1623)	2 (2–3)	12 (9–17)	74 (56–111)	517 (389–770)	76 (58–114)	5.1 (3.8–7.5)	5.3 (4.0–7.8)	5.3 (4.0–7.8)	5.0 (3.7–7.4)	5.1 (3.8–7.5)
75–120,000 inhabitants (*n* = 26)	14 (11–21)	102 (77–152)	494 (372–735)	1202 (904–1791)	1812 (1364–2699)	2 (2–4)	12 (9–18)	73 (55–109)	506 (381–754)	77 (58–115)	5.7 (4.3–8.5)	5.5 (4.1–8.2)	5.3 (4.0–7.9)	5.0 (3.8–7.4)	5.1 (3.8–7.6)
≥120,000 inhabitants (*n* = 27)	58 (44–87)	485 (365–721)	2482 (1869–3692)	5961 (4488–8873)	8986 (6766–13,373)	2 (2–4)	14 (10–21)	93 (70–138)	618 (465–919)	93 (70–139)	6.5 (4.9–9.6)	6.5 (4.9–9.6)	6.5 (4.9–9.7)	6.3 (4.7–9.3)	6.3 (4.8–9.4)
Non provincial capitals (*n* = 3615)	132 (99–196)	999 (752–1488)	4735 (3564–7053)	10,190 (7667–15,186)	16,056 (12,083–23,923)	2 (2–3)	11 (8–16)	66 (50–98)	460 (346–685)	63 (47–94)	4.8 (3.6–7.2)	4.7 (3.6–7.0)	4.7 (3.5–6.9)	4.4 (3.3–6.6)	4.5 (3.4–6.7)
<1000 inhabitants (*n* = 454)	1 (1–1)	6 (4–9)	31 (24–47)	79 (59–118)	117 (87–175)	1 (1–2)	6 (4–9)	35 (26–53)	250 (188–376)	41 (30–61)	2.4 (1.8–3.6)	2.3 (1.7–3.4)	2.2 (1.6–3.3)	2.1 (1.6–3.2)	2.1 (1.6–3.2)
1–2000 inhabitants (*n* = 592)	2 (2–4)	20 (15–30)	100 (75–150)	262 (196–393)	385 (289–577)	1 (1–2)	6 (5–10)	39 (29–58)	302 (227–454)	44 (33–66)	2.6 (1.9–3.9)	2.5 (1.9–3.8)	2.6 (2.0–3.9)	2.6 (2.0–3.9)	2.6 (2.0–3.9)
2–5000 inhabitants (*n* = 1049)	13 (10–20)	98 (73–146)	469 (352–702)	1089 (818–1629)	1669 (1254–2496)	2 (1–2)	8 (6–12)	47 (35–70)	347 (260–518)	48 (36–72)	3.4 (2.6–5.1)	3.4 (2.5–5.0)	3.3 (2.5–4.9)	3.2 (2.4–4.8)	3.3 (2.4–4.9)
≥5000 inhabitants (*n* = 1520)	115 (87–172)	876 (659–1303)	4134 (3113–6153)	8760 (6594–13,046)	13,886 (10,453–20,675)	2 (2–3)	11 (8–17)	71 (54–106)	491 (370–731)	67 (50–99)	5.2 (3.9–7.8)	5.1 (3.8–7.6)	5.0 (3.8–7.5)	4.8 (3.6–7.1)	4.9 (3.7–7.2)

The exposure-response function per increment of 0.1 NDVI is a RR for all-cause mortality of 0.96 (95% CI 0.94–0.97)[11]. Population data from GHSL are available at: https://ghsl.jrc.ec.europa.eu/download.php?ds=pop (Global Human Settlement Layer. GHS population grid (R2023). Product: GHS-POP, epoch: 2020, resolution: 100 m, coordinate system: Mollweide). NDVI data from Sentinel-2 are available at: https://code.earthengine.google.com (European Union. Copernicus Programme. Sentinel-2 mission. Image collection: 'COPERNICUS/S2_SR_HARMONIZED').

CI confidence interval, *HIA* health impact assessment, *NDVI* normalized difference vegetation index, *PWE* population-weighted exposure, *RR* relative risk.

https://doi.org/10.1038/s41467-024-54388-7

Table 3 | Estimated preventable years of life lost in the municipalities included in the HIA when using as counterfactual exposure (*k*) the 75th population-weighted percentile of greenest period NDVI in all the 300 m population-buffers. Italy, 2022

N = 3720 municipalities with a PWE to greenest period NDVI < 75th percentile (*k* = 0.46)	Preventable years of life lost														
	Number (95% CI)					Rate (95% CI) [per 100,000 inhabitants]					Rate fraction (95% CI) [%]				
	20–39 years	40–59 years	60–79 years	≥80 years	≥20 years	20–39 years	40–59 years	60–79 years	≥80 years	≥20 years	20–39 years	40–59 years	60–79 years	≥80 years	≥20 years
Italy (*n* = 3720)	11,103 (8359–16,526)	52,266 (39,345–77,819)	121,903 (91,762–181,518)	94,052 (70,780–140,116)	279,324 (210,247–415,980)	107 (81–160)	357 (269–532)	1090 (820–1623)	2575 (1938–3836)	702 (528–1045)	5.2 (3.9–7.7)	5.1 (3.9–7.7)	5.1 (3.8–7.6)	4.9 (3.7–7.3)	5.0 (3.8–7.5)
Provincial capitals (*n* = 105)	4322 (3254–6432)	21,042 (15,844–31,316)	51,132 (38,498–76,102)	41,761 (31,434–62,190)	118,257 (89,030–176,040)	118 (89–175)	407 (306–605)	1269 (956–1889)	2907 (2188–4329)	826 (622–1230)	5.9 (4.5–8.8)	6.0 (4.5–8.9)	5.9 (4.5–8.9)	5.7 (4.3–8.5)	5.9 (4.4–8.7)
<45,000 inhabitants (*n* = 27)	180 (135–270)	764 (573–1145)	1901 (1426–2849)	1643 (1232–2463)	4487 (3366–6727)	82 (62–124)	242 (182–363)	702 (527–1053)	1716 (1287–2572)	498 (374–747)	3.5 (2.6–5.2)	3.4 (2.5–5.1)	3.4 (2.5–5.1)	3.3 (2.5–5.0)	3.4 (2.5–5.1)
45–75,000 inhabitants (*n* = 25)	405 (305–603)	1847 (1391–2749)	4571 (3442–6802)	3557 (2678–5295)	10,380 (7816–15,448)	110 (83–165)	365 (275–543)	1101 (829–1638)	2576 (1940–3835)	728 (548–1084)	5.0 (3.8–7.5)	5.2 (3.9–7.8)	5.2 (3.9–7.8)	5.0 (3.8–7.4)	5.1 (3.9–7.6)
75–120,000 inhabitants (*n* = 26)	726 (547–1080)	3212 (2418–4780)	7354 (5536–10,951)	6062 (4562–9034)	17,355 (13,063–25,845)	121 (91–180)	379 (286–565)	1094 (824–1629)	2553 (1921–3804)	736 (554–1097)	5.7 (4.3–8.5)	5.5 (4.1–8.2)	5.3 (4.0–7.8)	5.0 (3.8–7.5)	5.2 (3.9–7.8)
≥120,000 inhabitants (*n* = 27)	3011 (2267–4479)	15,219 (11,461–22,643)	37,305 (28,094–55,500)	30,500 (22,963–45,398)	86,035 (64,785–128,020)	121 (91–180)	434 (327–646)	1397 (1052–2078)	3160 (2379–4703)	893 (673–1329)	6.5 (4.9–9.6)	6.4 (4.9–9.6)	6.5 (4.9–9.6)	6.3 (4.7–9.3)	6.4 (4.8–9.5)
Non provincial capitals (*n* = 3615)	6781 (5105–10,094)	31,224 (23,501–46,503)	70,771 (53,265–105,417)	52,290 (39,346–77,927)	161,066 (121,217–239,940)	102 (77–151)	330 (249–492)	989 (744–1473)	2359 (1775–3516)	632 (476–941)	4.8 (3.6–7.2)	4.7 (3.5–7.0)	4.6 (3.5–6.9)	4.4 (3.3–6.6)	4.6 (3.4–6.8)
<1000 inhabitants (*n* = 454)	43 (32–65)	177 (133–266)	474 (355–713)	382 (287–575)	1077 (807–1619)	66 (49–99)	178 (134–268)	530 (397–797)	1220 (914–1833)	376 (282–566)	2.4 (1.8–3.6)	2.3 (1.7–3.4)	2.2 (1.6–3.3)	2.1 (1.6–3.2)	2.2 (1.6–3.3)
1–2000 inhabitants (*n* = 592)	126 (95–189)	622 (466–932)	1510 (1133–2264)	1309 (982–1963)	3567 (2676–5349)	59 (44–88)	201 (151–301)	583 (437–874)	1512 (1134–2267)	410 (308–615)	2.6 (1.9–3.9)	2.5 (1.9–3.8)	2.6 (1.9–3.9)	2.6 (2.0–3.9)	2.6 (1.9–3.9)
2–5000 inhabitants (*n* = 1049)	673 (506–1006)	3056 (2296–4570)	7076 (5315–10,582)	5510 (4139–8240)	16,315 (12,255–24,398)	76 (57–114)	240 (180–359)	708 (532–1060)	1754 (1317–2622)	470 (353–703)	3.3 (2.5–5.0)	3.4 (2.5–5.0)	3.3 (2.4–4.9)	3.2 (2.4–4.8)	3.3 (2.5–4.9)
≥5000 inhabitants (*n* = 1520)	5938 (4472–8833)	27,369 (20,607–40,735)	61,712 (46,462–91,858)	45,089 (33,939–67,149)	140,108 (105,479–208,574)	108 (81–160)	352 (265–525)	1062 (800–1581)	2527 (1902–3763)	672 (506–1000)	5.2 (3.9–7.8)	5.1 (3.8–7.5)	5.0 (3.8–7.4)	4.7 (3.6–7.1)	4.9 (3.7–7.3)

The exposure-response function per increment of 0.1 NDVI is a RR for all-cause mortality of 0.96 (95% CI 0.94–0.97)[11]. Population data from GHSL are available at: https://ghsl.jrc.ec.europa.eu/download.php?ds=pop (Global Human Settlement Layer. GHS population grid (R2023). Product: GHS-POP, epoch: 2020, resolution: 100 m, coordinate system: Mollweide). NDVI data from Sentinel-2 are available at: https://code.earthengine.google.com (European Union. Copernicus Programme. Sentinel-2 mission. Image collection: 'COPERNICUS/S2_SR_HARMONIZED').

CI confidence interval, *HIA* health impact assessment, *NDVI* normalized difference vegetation index, *PWE* population-weighted exposure, *RR* relative risk.

Table 4 | Relationship between the PWEs to relative land cover measures and the PWE to greenest period NDVI. Spearman rank correlations and GAMMs. Italy, 2021 (land cover) and 2022 (NDVI)

N = 7904 municipalities	Spearman rank correlations		GAMMs with cubic regression splines, province random effects, and population weights			
Exposures [log of PWE]	**ρ**	**95% CI**	**EDF**	**Adj. R^2**	**Deviance explained**	***P*-value**
Tree cover, proportion	0.77	0.76; 0.78	7.85	0.82	0.84	<0.001
Shrubland, proportion	−0.02	−0.04; 0.00	–	–	–	–
Grassland, proportion	0.15	0.13; 0.17	6.02	0.63	0.66	<0.001
Green area, proportion	0.86	0.85; 0.87	7.20	0.91	0.93	<0.001
Tree cover, proportion; Grassland, proportion	–	–	8.50; 6.32	0.92	0.93	<0.001; <0.001
Built-up, proportion	−0.87	−0.88; −0.87	7.94	0.93	0.94	<0.001
Tree cover, ratio to built-up	0.87	0.86; 0.87	7.83	0.89	0.91	<0.001
Shrubland, ratio to built-up	0.07	0.05; 0.09	–	–	–	–
Grassland, ratio to built-up	0.57	0.56; 0.59	5.46	0.76	0.79	<0.001
Green area, ratio to built-up	0.89	0.89; 0.90	7.63	0.94	0.95	<0.001
Tree cover, ratio to built-up; Grassland, ratio to built-up	–	–	7.57; 7.20	0.93	0.94	<0.001; <0.001

Population data from GHSL are available at: https://ghsl.jrc.ec.europa.eu/download.php?ds=pop (Global Human Settlement Layer. GHS population grid (R2023). Product: GHS-POP, epoch: 2020, resolution: 100 m, coordinate system: Mollweide). NDVI data from Sentinel-2 are available at: https://code.earthengine.google.com (European Union. Copernicus Programme. Sentinel-2 mission. Image collection: 'COPERNICUS/S2_SR_HARMONIZED'). Land cover data from WorldCover are available at: https://code.earthengine.google.com (European Space Agency. WorldCover Project. 2021. Image collection: 'ESA/WorldCover/v200').

Adj. R^2 adjusted R^2, *CI* confidence interval, *EDF* estimated degrees of freedom, *GAMMs* generalised additive mixed effects models, *Log* natural logarithm, *NDVI* normalized difference vegetation index, *PWE* population-weighted exposure.

European regions and 8–12 K lower in Central European regions. The overall effectiveness of treeless urban green spaces in reducing temperatures is lower, and their cooling impact is roughly 2–4 times less than that of urban trees[54]. Trees not only block the sun's rays from reaching people by providing shade, but they also limit the amount of heat that impermeable materials with high heat capacity and thermal conductivity, such as concrete, can absorb from the sun. Vegetation can increase urban albedo relative to black asphalt surfaces, and when compared to impermeable surfaces of the same albedo, vegetated surfaces have lower radiative temperatures[45,55–57].

Examples of greening interventions include the regeneration of urban areas (turning former industrial areas into urban parks), the increase of nature-based solutions in existing buildings (green roofs and vertical gardens), the reorganisation of traffic and the reallocation of road and parking space to green and natural areas (green belt and corridors), and the general greening of the city with more street trees, green corridors, and pocket parks[28].

Our results show discrepancies between classes of municipalities, with higher impacts in provincial capitals with 120,000 inhabitants or more (6.3% of mortality). The groups of municipalities showing lower (<3.5% of mortality) health impacts were non provincial capitals with less than 5000 inhabitants and provincial capitals with less than 45,000 inhabitants. It is important to carry out assessments for all municipalities and inhabitants, not only for selected or larger cities. In this work, we have carried out a national assessment by using large-scale data and setting a statistical, nationwide population-based target. This also ensures comparability of the estimates. However, these aspects, which are the main strengths of the study, could also be a source of concern as we lack local information and data on the practical applicability of the NDVI target in each municipality in terms of interventions and characteristics of greenness. The counterfactual exposure to greenness is statistically determined at the national level and represents a generic target that may be too high for some municipalities and too low for others. Therefore, it may be desirable in the future to also carry out assessments that are more adapted to the local context. These specific studies and targeted interventions are necessary to achieve the highest possible level of greenery in each area, compatible with the local geographical, climatic, floristic, urban, architectural, and cultural characteristics.

Adaptation to climate change and urban green spaces are closely linked. Heat-related morbidity in cities is a major public health concern. The urban heat island effect can pose serious health risks during heat waves and extreme heat events. Urban green spaces, such as parks, street trees, and green roofs, can mitigate these effects with an estimated cooling effect of 1°. Trees can provide shade in warmer weather and reduce the need for air conditioning. In warmer countries, they can also provide comfortable outdoor spaces and help people avoid heat-related stress. Mitigating the urban heat island may partly explain the benefits of green spaces on mortality. Therefore, future avoidable deaths from the implementation of urban greening could potentially be even greater if we take into account future, increased baseline temperature-related deaths[1,11,28,58–60]. It would therefore be interesting to extend this research study in the future with scenarios of attributable deaths due to climate change[58,59].

Strengths of the present study are the inclusion of all municipalities and population of a country, the use of ultra-fine resolution satellite data for exposure, the use of the WHO and Konijnendijk criteria of 300 m for assessing the presence of residential greenness, the implementation of the population-weighted approach to account for the differences in the spatial distribution of the population in different areas, the use of recent exposure, population and mortality data, the use of city-specific and age-specific mortality data, the stratified analysis by municipality groups and age groups, the use of the same counterfactual exposure based on real data in all municipalities for comparability purposes, the approximate compliance of this counterfactual with the 30–300 part of the 3–30–300 rule, the analyses of land cover, and the application of several sensitivity analyses for populations, targets, functions, formulas and statistical models.

In addition, our method is easily replicable without the need for georeferencing the local population. The PWE approach allows exposure to be estimated at the municipal level using public exposure and population data, which are freely available worldwide at high resolution. The required information on mortality and population are aggregated at the municipal level. Using the most recent statistical data, the HIA can be replicated worldwide. Furthermore, the implementation of various sensitivity analyses allows the comparison of impacts assessed using different methods and scenarios.

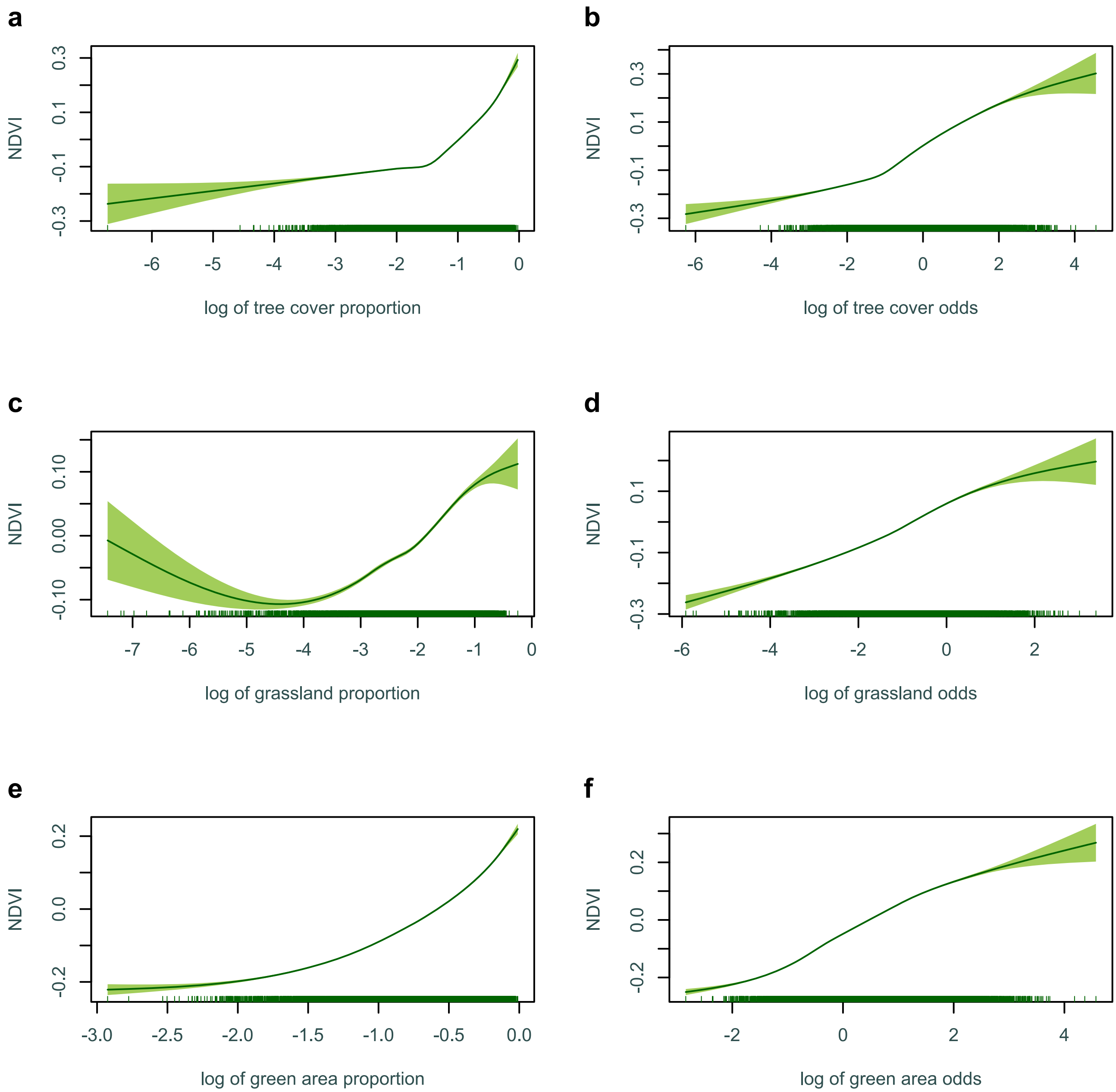

Fig. 3 | Relationship between the PWEs to relative land cover measures and the PWE to greenest period NDVI. The plots show the smooth functions as estimated by the single-predictor GAMMs. The shaded areas show confidence bands at 2 standard errors above and below the estimates. Rug plots show the distribution of the data. Italy, 2021 (land cover) and 2022 (NDVI). a, **c** and **e**: one model for each proportion measure. **b**, **d** and **f**: one model for each ratio-to-built-up (odds) measure. GAMMs: generalised additive mixed effects models. Log: natural logarithm. NDVI: normalized difference vegetation index. PWE: population-weighted exposure. Plot created with R version 4.2.3. Population data from GHSL are available at: https://ghsl.jrc.ec.europa.eu/download.php?ds=pop (Global Human Settlement Layer. GHS population grid (R2023). Product: GHS-POP, epoch: 2020, resolution: 100 m, coordinate system: Mollweide). NDVI data from Sentinel-2 are available at: https://code.earthengine.google.com (European Union. Copernicus Programme. Sentinel-2 mission. Image collection: 'COPERNICUS/S2_SR_HARMONIZED'). Land cover data from WorldCover are available at: https://code.earthengine.google.com (European Space Agency. WorldCover Project. 2021. Image collection: 'ESA/WorldCover/v200').

On the flip side, there are also limitations that are essentially shared with the other published studies on NDVI and mortality[2–11,27,28]. The first is the limitation, common to most of environmental epidemiology studies, of using residential exposure as a proxy for overall individual exposure, even though people spend only part of their time at home. However, the 300-m approach employed in the present HIA can somewhat extend the exposure observation to areas around the house within a radius of 300 m. Therefore, the PWE method using these buffers could also consider the average exposure to greenness near homes[1,11,26,28].

A second limitation is that the assessment does not take into account the quality or use of green spaces, nor the specific characteristics of the areas analysed. Basically, it is assumed that all green spaces measured by the NDVI are qualitatively homogeneous and equally accessible to all residents in the buffer centroid. Instead, urban green spaces have different components that influence their quality and shape the patterns of use, time spent, and interactions with these spaces among different population subgroups[28]. Key attributes of green spaces, such as safety, aesthetics, amenities and maintenance are crucial in promoting outdoor physical activity. Negative aspects

https://doi.org/10.1038/s41467-024-54388-7

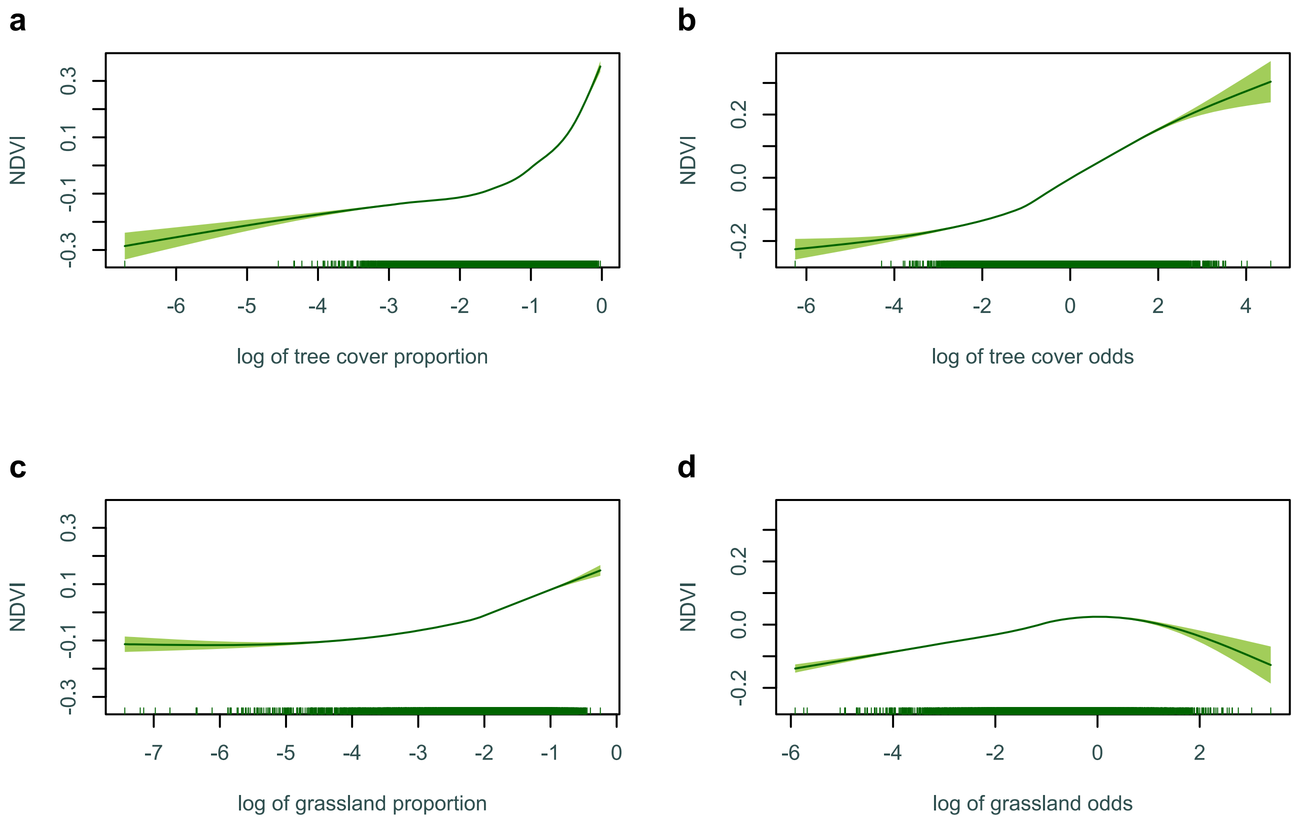

Fig. 4 | Relationship between the PWEs to relative land cover measures and the PWE to greenest period NDVI. The plots show the smooth functions as estimated by the multiple-predictor GAMMs. The shaded areas show confidence bands at 2 standard errors above and below the estimates. Rug plots show the distribution of the data. Italy, 2021 (land cover) and 2022 (NDVI). a and **c**: one model for multiple proportion measures. **b** and **d**: one model for multiple ratio-to-built-up (odds) measures. GAMMs: generalised additive mixed effects models. Log: natural logarithm. NDVI: normalized difference vegetation index. PWE: population-weighted exposure. Plot created with R version 4.2.3. Population data from GHSL are available at: https://ghsl.jrc.ec.europa.eu/download.php?ds=pop (Global Human Settlement Layer. GHS population grid (R2023). Product: GHS-POP, epoch: 2020, resolution: 100 m, coordinate system: Mollweide). NDVI data from Sentinel-2 are available at: https://code.earthengine.google.com (European Union. Copernicus Programme. Sentinel-2 mission. Image collection: 'COPERNICUS/S2_SR_HARMONIZED'). Land cover data from WorldCover are available at: https://code.earthengine.google.com (European Space Agency. WorldCover Project. 2021. Image collection: 'ESA/WorldCover/v200').

such as safety concerns, graffiti, vandalism, litter, noise, pollution, and dog fouling discourage park use and physical activity. Studies suggest that access to attractive, large public open spaces is associated with higher levels of walking[61–65]. The quality of green spaces, characterised by accessibility, maintenance, absence of litter, and safety, is positively associated with general health. The ability of green spaces to provide relaxation and recreation has been identified as crucial to mental well-being. Eight sensory dimensions of urban parks have been identified: serene, space, nature, rich in species, refuge, culture, prospect, and social. Refuge and nature are strongly linked to reduced stress. Refuge is a safe, enclosed area for play and observation, while nature provides a sense of being in the wild. Access to serene spaces significantly reduce the risk of mental illness. In addition, views of trees and grass from homes prevent aggression and mental fatigue compared with barren views[66–74]. In general, the methodology of this health impact assessment is focused on the quantitative analysis of the greenest period NDVI rather than on the qualitative assessment of green spaces. However, conducting studies on entire nations has these challenging limitations. To go into more detail and consider the quality of green spaces, it may be necessary to restrict the study to a limited number of municipalities and include additional local-level variables. Furthermore, translating these analyses into health impacts requires specific exposure-response functions that are not currently available. Future research could benefit from incorporating methods that explicitly categorise and qualify different types of green space to better understand their unique roles and impacts in different settings.

A third limitation is the assumption of homogeneity in the effect of urban greenery on mortality across different age groups, sexes, socioeconomic indicators, and types of human settlements according to the degree of urbanisation. In fact, we assume that the relative risk for given NDVI increments is the same in all these categories. However, we do not have solid evidence that the exposure-response function between NDVI and mortality is not homogeneous to use this information in a reliable assessment. With regard to age, one of the studies included in the meta-analysis reported a lower RR in older people compared with the pooled estimate from the meta-analysis in all age groups[7,11]. Conversely, another study in the meta-analysis seemed to show a more protective effect in younger age groups[2]. Therefore, we have reported two different sensitivity analyses for the two scenarios. We have also performed a sensitivity analysis for possible differences according to the degree of urbanisation. Further research is therefore needed to investigate the possible heterogeneity of the effect in more detail.

A fourth limitation is the assumption that the exposure-response function is linear. This is consistent with the assumption of linearity of the exposure-response function reported in the meta-analysis[11]. Although all cohort studies included in the meta-analysis[2–10] reported RRs for continuous green space exposure, we are not sure that the exposure-response function is strictly linear[11]. However, most of the studies included in the meta-analysis had also examined the functional forms and reported an essentially linear relationship[2,4–6,10]. Some of these studies also showed the plotted functional forms of the estimated relationship between greenest period NDVI and mortality[2,6].

https://doi.org/10.1038/s41467-024-54388-7

Our study examined the health impacts of positive greenest period NDVI values up to a counterfactual of 0.46, a relatively limited range in which the linearity assumption appears to hold according to the plots. Finally, other studies have also reported a linear relationship between green space and human health[75–77]. However, we hope that future research can further investigate possible non-linear relationships between greenness and mortality.

The assumptions about homogeneity and linearity are also consistent with the approach used in this HIA, which is based on the guidance provided in various scientific papers and official documents[28,33–43,78–86]. For example, the same framework (use of metanalytic RRs to estimate health impacts) and assumptions (linearity of the exposure-response function and homogeneity of the effect) were reported by the WHO also in the officially provided tools for air quality HIA (AirQ+)[85]. The WHO HRAPIE (Health risks of air pollution in Europe) document on exposure-response functions for air pollutants[86] recommended the same approach and basically provided a list of available metanalytic RRs to be used in HIA, based on the same assumptions mentioned above. Therefore, this methodological part of the work (HIA design and assumptions in the use of the exposure-response function) is basically a standard and well referenced approach in HIA[28,33–43,78–86]. However, further research is essential and recommended for the future to explore these associations in more detail and to provide more accurate and tailored risk functions to enable more accurate assessments. With these perspectives in mind, the exposure-response function used in the present study[11] is currently the most recent and robust estimate available in the literature for conducting a reliable health impact assessment.

In conclusion, we estimate in this study that 5% of all deaths and years of life lost in Italy could be prevented by greening residential areas up to the level of greenness currently achieved by the 25% of the population. More green means fewer deaths, thus strong action is needed to increase the amount and accessibility of green spaces in all human settlements.

Methods

Design, analysis, and study area

This is a quantitative health impact assessment study. Data analysis and visualisation were carried out using Google Earth Engine, R version 4.2.3 and QGIS version 3.28.4. The study area corresponds to all the Italian municipalities, regardless of size or population, as reported by the Italian National Institute for Statistics (ISTAT). Municipalities can be classified as provincial capitals or not, and according to their population. For the year 2022, the ISTAT list includes 7,904 municipalities, 109 provincial capitals and 7,795 non provincial capitals. On 31 December 2022, the total resident adult population (aged ≥20 years) was 48,628,328: 14,530,259 in provincial capitals and 34,098,069 in non provincial capitals[87–89].

Internal review board approval

This study is neither analytical nor individual. It is a municipality-level health impact assessment that attempts to estimate the impact of a hypothetical greening intervention using public data and functions. This is a commonly used methodology in public health and generally does not require ethical approval. However, we submitted a request to the scientific secretariat of the local ethics committee asking if their opinion was required for the study. After evaluating the manuscript, they replied that an internal review board approval is not required for this type of study, because it does not involve human subjects and relies on public mortality counts at the municipal level to assess the impact of an environmental intervention.

Population and baseline outcome data

The total number of inhabitants per grid cell was obtained from the Global Human Settlement (GHS) population grid for 2020 with a resolution of 100 m. This spatial raster product ('GHS-POP_GLOBE_R2023') depicts the distribution of residential population, expressed as the number of people per cell[90–93]. Pixels with no population were treated as no-data and excluded from the analysis. The population raster was converted into a vector layer of points and the information on the Italian administrative units were spatially joined from the vector of polygons of the ISTAT municipalities[87]. Non-Italian population points (i.e., points with no joined attributes) were excluded. This vector of population-points was used for the exposure assessment.

The GHS population was used to calculate the weighted percentiles and means of the buffer-level exposures (see the section 'Baseline exposure'). The adult (≥20 years) and age-specific (5-year age groups, 20–24, 25–29,…,95–99, ≥100) municipal ISTAT population was used to calculate the age-specific rates, to classify the municipalities by number of inhabitants, and to calculate the weighted percentiles and means of the municipal level exposures and populations[88,89]. The Spearman rank correlation between the GHS and ISTAT populations at the municipal level was > 0.99.

The number of all-cause baseline deaths (BD) for each age group of the adult population in 2022 by municipality was obtained from a public ISTAT dataset[94]. The number of all-cause baseline years of life lost (BYLL) for each age group of the adult population in 2022 by municipality was estimated by multiplying the number of baseline deaths in the age group by the central age (3rd year of the age group) province-specific life expectancy reported by ISTAT[95].

Baseline exposure

The baseline exposure is the actual level of greenness as measured by the greenest period NDVI. We calculated the NDVI at a resolution of 10 m using images from the Sentinel-2 mission of the European Union's Copernicus Programme via Google Earth Engine (image collection: 'COPERNICUS/S2_SR_HARMONIZED'). Sentinel-2 is a constellation of two satellites with a minimum combined revisit time of 5 days[96].

All images collected for Italy[87] between 1 April and 30 June 2022 were included to ensure the greenest period of the year. The NDVI is not an exposure itself, but rather an index proxy of the real exposure, which is the green space. For simplicity, we have referred to it in the text as 'PWE to greenest period NDVI', but the full expression should be 'PWE to greenness throughout the year, assessed using the greenest period NDVI'[28]. A more detailed description of this approach is reported in the Supplementary Note 2. A 5 km buffer was added to the entire study area to avoid loss of exposure information at the boundaries. Images with a granule-specific cloudy pixel percentage of 20% or more were removed (images of lower quality). The selected images were also masked using the 'QA60' bitmask band information to remove pixels with opaque clouds and cirrus clouds.

Then, for each image time t in a pixel space s, the NDVI ($NDVI_{t_s}$) is estimated according to Eq. (1):

$$\mathrm{NDVI}_{t_s} = \frac{\mathrm{NIR}_{t_s} - \mathrm{Red}_{t_s}}{\mathrm{NIR}_{t_s} + \mathrm{Red}_{t_s}} \quad (1)$$

where NIR_{t_s} and Red_{t_s} refer to the spectral reflectances of the pixel at a specific time t in a specific space s measured in the near infrared (833–835 nm) and red (665 nm) wavebands respectively. The calculation of the NDVI always results in a number that ranges from −1 to 1, with positive and higher values indicating more greenness[11,13]. For each pixel space s in the study region, a reduction of the NDVI measures was obtained by calculating the temporal arithmetic mean ($NDVI_s$) of all the NDVI values of the corresponding pixels across the images in the temporal line ($NDVI_{t_s}$). To account for the possible beneficial effects of the blue areas on human health, the pixels corresponding to permanent water bodies (see the section 'Analysis of land cover') were excluded (masked out) from the exposure assessment[28].

https://doi.org/10.1038/s41467-024-54388-7

In line with the WHO's and Konijnendijk's recommendations[1,26], the exposure to NDVI value was estimated by adding a circular buffer of 300 m radius around each population-point to indicate the proximity to greenness (i.e., about 5 min walk along walkable pathways)[28]. For each population-buffer p, the spatial arithmetic mean ($NDVI_p$) of the temporally averaged NDVI values of all the pixels within the population-buffer ($NDVI_{s_p}$) was calculated. Basically, a population-buffer was created for each inhabited point, with the point-derived (central population-point) information of population count and administrative division (municipality and province), and the circle-area-derived (surrounding population-buffer) information of temporally and spatially averaged NDVI.

For each municipality-area a, the PWE to greenest period NDVI (PWE_a) was calculated as a weighted mean of the temporally and spatially averaged NDVI values ($NDVI_{p_a}$) of the population-buffers p_a whose centroid is included in the municipality-area a. For each included population-buffer p_a, the weight was the GHS population (POP_{p_a}) of the centroid, as shown in Eq. (2)[31,33,97].

$$PWE_a = \sum_{p_a}(NDVI_{p_a} \times POP_{p_a}) / \sum_{p_a}(POP_{p_a}) \tag{2}$$

This approach allows exposure to be weighted by population and has been used in other studies on air pollution[33,35,36,39–41,97]. To take in consideration the influence of sparsely populated areas[28], sensitivity analyses were performed including only the population-buffers with a population count greater than 2. We also reported an uncertainty analysis for the baseline exposure assessment and sensitivity analyses for the choice of the greenest period and satellite. Further details are provided in the Supplementary Notes 1 and 2, respectively.

Counterfactual exposure

The counterfactual exposure is the level of greenness that needs to be achieved to prevent the deaths estimated in the health impact assessment, i.e. a target level of exposure to greenness. There are no specific recommendations for NDVI values when setting the counterfactual exposure. It may be desirable to conduct these assessments using the same counterfactual exposure for all areas to assure comparability. This target exposure should be population-based, realistically achievable in some way, and possibly linked to the current green space recommendations.

We proposed a population-weighted approach. Using a methodology consistent with that chosen for baseline exposure, the counterfactual level of exposure to green space was set as the 75th population-weighted percentile of the population-buffers' greenest period NDVI. We used the 75th population-weighted percentile as a conservative measure to try to make the target realistically achievable. This means that 75% of the Italian population was exposed to a buffer-level mean NDVI in the period April-June 2022 that was lower than the counterfactual level. Or, to say in other words, that 25% of the Italian population was exposed to a buffer-level greenest period NDVI that was higher than the counterfactual level, thus achieving the target. In the study area, this counterfactual greenest period NDVI value is 0.46 and corresponds to an average of 30% tree cover within a 300-m radius buffer around the residence. Specifically, selecting only those municipalities with a PWE to greenest period NDVI in the range 0.46 ± 0.01, we found an overall PWE to tree cover proportion of 30% (see the section 'Analysis of land cover')[1,26].

This approach has several advantages. First, it could evaluate green targets that are statistically based on real exposures and populations. Second, it ensures comparability across all municipalities. Third, it is likely to be quite robust to errors in exposure assessment, as hypothetical shifts in baseline exposure measures could be propagated to the percentile-based target, making the expected difference similar. Finally, the target in the study area approximately complies with the 30–300 part of the 3–30–300 rule[26].

We used sensitivity analyses to explore possible changes in impact estimates by setting alternative counterfactual exposures. Specifically, we used as alternative counterfactual exposures the 75th population-weighted percentile of the municipality-level PWEs to greenest period NDVI and the 75th unweighted percentiles of both municipality-level PWEs to greenest period NDVI and buffer-level greenest period NDVI. The first target implies that 75% of the Italian population was exposed to a municipality-level (PWE) mean NDVI in the period April-June 2022 that was lower than the counterfactual level. The interpretation of the unweighted percentiles counterfactuals is analogue to the weighted percentiles ones: it means that in the period April-June 2022 the population of 75% of the Italian municipalities or population-buffers was exposed to a municipality-level (PWE) or buffer-level mean NDVI value that was lower than the counterfactual level, respectively. We performed further sensitivity analyses using the 50th and the 95th population-weighted percentiles as counterfactual exposures. We also reported an uncertainty analysis for the counterfactual exposure assessment and sensitivity analyses for the choice of the greenest period and satellite. Further details are provided in the Supplementary Notes 1 and 2, respectively.

Exposure-response function

We used the exposure-response function from the systematic review and meta-analysis by Rojas-Rueda et al.[11]. The review included only cohort studies and estimated that the RR for all-cause mortality per 0.1 NDVI increase within a buffer of 500 m or less from homes was 0.96 (95% CI 0.94–0.97).

Although this exposure-response function is the most recent and reliable estimate to date, sensitivity analyses were performed to assess how the results might vary with alternative functions. Specifically, the relative risks from the two studies with the higher[7] and lower[4] weight in the meta-analysis[11] were used as alternative exposure-response functions. In addition, to account for the possible heterogeneity of the effects between different age groups[2,7,11], two sensitivity analyses were performed, one using a different exposure-response function for the population aged ≥80 years (greater protective effect compared with the meta-analytic estimate)[7,11] and the other testing a + 50% of protective effect in the population aged <80 years. Finally, to take into account the possible heterogeneity of the effect between different types of municipalities[4,6,7,11], we performed a sensitivity analysis considering a 20% reduction in the protective effect in non provincial capital municipalities. This value was calculated as a weighted average of the estimated effect reduction in rural areas, using information from some of the studies in the meta-analysis[4,6,7,11]. The weights were the same as those used in the meta-analysis[11]. To be conservative, we have applied this 20% reduction to all non provincial capital, although not all of them can be considered rural[87–89].

Health impact assessment

A quantitative health impact assessment at the municipal level was conducted to estimate the impact on all-cause mortality of increasing the exposure to greenness up to the counterfactual value[11,27–43]. For each municipality-area a, the exposure difference (Δ_a) between the counterfactual (k) and the baseline (PWE_a) greenest period NDVI exposure level was calculated. For each municipality-area a, the relative risk for the exposure difference (RR_a) and the preventable fraction (PF_a) were estimated using the exposure-response function ($RR_{0.1}$) with its confidence interval[11], as shown in Eqs. (3) and (4)[29,34,35]:

$$RR_a = \exp(\ln(RR_{0.1}) \times 10 \times \Delta_a) \tag{3}$$

$$PF_a = 1 - RR_a \tag{4}$$

https://doi.org/10.1038/s41467-024-54388-7

For each municipality-area a and five-year age group j, the number of preventable deaths ($PD_{a,j}$) and preventable years of life lost ($PYLL_{a,j}$) was estimated, using the municipality and age-specific baseline deaths ($BD_{a,j}$) and years of life lost ($BYLL_{a,j}$), as shown in Eqs. (5) and (6)[27,29–35,37,38]:

$$PD_{a,j} = PF_a \times BD_{a,j} \tag{5}$$

$$PYLL_{a,j} = PF_a \times BYLL_{a,j} \tag{6}$$

Sensitivity analyses were performed using an alternative approach in calculating the preventable fractions. The full explanation of the formulas used in the two approaches is given in the Supplementary Note 3.

Presentation of the assessments' results

Municipalities were classified according to whether they were provincial capitals or not and according to their population size. The population categories were chosen according to their rounded, unweighted quartiles specific to provincial capitals and non provincial capitals. The five-year age groups were combined into four main age groups (20–39, 40–59, 60–79, and ≥80 years). Results were reported for all the municipalities with a preventable fraction > 0, corresponding to a PWE to greenest period NDVI below the counterfactual exposure. The estimated impact measures were summed by municipality group and age group and reported as preventable numbers (PD or PYLL), preventable rates (the ratio of the preventable numbers to the ISTAT population, per 100,000) and preventable rate fractions (the ratio of the preventable rates to the baseline rates). These preventable (rate) fractions were calculated for each group using the health impact estimates and can be interpreted as the fractions of the baseline deaths or YLL that could be avoided by achieving the counterfactual exposure level[29]. The PWEs to greenest period NDVI, difference between counterfactual exposure and greenest period NDVI, tree cover proportion and green area proportion (see the section 'Analysis of land cover') were calculated for each group of municipalities as a weighted mean of the respective PWEs of the municipalities included. For each municipality, the weight was the ISTAT population.

Analysis of land cover

We retrieved via Google Earth Engine the latest available land cover information for Italy[87] from the European Space Agency (ESA) WorldCover 10 m 2021 product (image collection: 'ESA/WorldCover/v200'), which provides a global map for 2021 at 10 m resolution based on Sentinel-2 and Sentinel-1 data. The product includes 11 land cover classes and has been generated in the framework of the ESA WorldCover Project, part of the 5th Earth Observation Envelope Programme of the ESA[98]. As with the NDVI assessment, a 5 km buffer around the national boundaries was added, and the land cover pixels classified as permanent water bodies were excluded from the analysis.

The classes analysed were tree cover, shrubland, grassland, green area (sum of the first three) and built-up. For each 300-m buffer, the proportion of a class was calculated as the ratio of the sum of the pixels in that class to the sum of all pixels. The PWEs to these proportion measures were calculated using the same methods described for the NDVI. Specifically, the PWE to the proportion of each green class was calculated for each municipality as the weighted mean of the proportion measure of the specific green class of the population-buffers whose centroid was included in the municipality itself. For each included population-buffer, the weight was the GHS population of the centroid. To quantify the presence of specific green classes in relation to the human built environment, the PWE to the ratio of each green class to built-up class (odds) was estimated for each municipality as the ratio of the PWE to the specific green class proportion and the PWE to the built-up proportion. To summarise, the calculated proportion measures (PWE) were the proportion of tree cover, shrubland, grassland, green area and built-up. The calculated ratio-to-built-up measures (PWE) were the ratio-to-built-up of tree cover, shrubland, grassland and green area.

Spearman ρ correlation coefficients were calculated at the municipal level between the natural logarithm of the PWE to each of the relative land cover measures (proportion and ratio-to-built-up of the analysed classes) and the PWE to the greenest period NDVI. Generalised additive mixed effect models were fitted at municipal level using the PWE to greenest period NDVI as the dependent variable and the natural logarithm of the PWEs to each of the relative land cover measures as the fixed effects predictors one at a time (single-predictor models: one model for each proportion measure and one model for each ratio-to-built-up measure) or in combination (multiple-predictor models: one model for multiple proportion measures and one model for multiple ratio-to-built-up measures). A cubic regression spline penalised by the conventional integrated square second derivative cubic spline penalty was chosen as smooth term for the relative land cover measures. In all models, the province was included as a random effect to account for the differences between the provinces, specifically as a parametric term penalised by a ridge penalty, which is equivalent to assuming that the coefficients are independent and identically distributed normal random effects. The GHS population was used as weight in the models. Restricted maximum likelihood was used as the smoothness selection method[99].

The effect of the relative land cover measure (smooth function) on the greenest period NDVI was plotted for each model. The plotted values of greenest period NDVI represent only the estimated effect of the relative land cover measure, and not the absolute values of the NDVI. In our models, this value depends on the intercept, the random effect of province, and the land cover measures. The shaded areas show confidence bands at 2 standard errors above and below the estimates. Rug plots show the distribution of the data. Sensitivity analyses were performed by choosing different smoothing terms (thin plate regression spline, cubic or thin plate regression spline with shrinkage, cubic b-spline or p-spline) or by fitting models without random effects and/or population weights[99].

Reporting summary

Further information on research design is available in the Nature Portfolio Reporting Summary linked to this article.

Data availability

The data used in this study are available in the following repositories. ISTAT administrative boundaries are available here: https://www.istat.it/it/archivio/222527. ISTAT Codes of administrative units are available here: https://www.istat.it/storage/codici-unita-amministrative/Elenco-comuni-italiani.xls. ISTAT population data are available here: https://demo.istat.it/app/?i=POS&l=it. GHS population data are available here: https://ghsl.jrc.ec.europa.eu/download.php?ds=pop. ISTAT deaths data are available here: https://www.istat.it/storage/dati_mortalita/Decessi-comunali-giornalieri-4-13122023.zip. ISTAT life expectancy data are available here: https://demo.istat.it/app/?i=TVM&l=it. Sentinel-2 data (image collection: 'COPERNICUS/S2_SR_HARMONIZED') and WorldCover data (image collection: 'ESA/WorldCover/v200') are available on Google Earth Engine: https://code.earthengine.google.com/. The data generated in this study have been deposited in the OSF database with the accession code GOV@v8.o3@hia: https://osf.io/wzsv7/?view_only=96c8c62ca3744794bbabb90ac77814c4.

Code availability

The codes used in this study have been deposited in the OSF database with the accession code GOV@v8.o3@hia: https://osf.io/wzsv7/?view_only=96c8c62ca3744794bbabb90ac77814c4.

References

1. World Health Organization. Urban green spaces and health. *World Health Organization Regional Office for Europe* (2016). https://apps.who.int/iris/handle/10665/345751 (Accessed: 18 July 2023).
2. Crouse, D. L. et al. Urban greenness and mortality in Canada's largest cities: a national cohort study. *Lancet Planet. Health* **1**, e289–e297 (2017).
3. Villeneuve, P. J. et al. A cohort study relating urban green space with mortality in Ontario, Canada. *Environ. Res.* **115**, 51–58 (2012).
4. James, P., Hart, J. E., Banay, R. F. & Laden, F. Exposure to greenness and mortality in a nationwide prospective cohort study of women. *Environ. Health Perspect.* **124**, 1344–1352 (2016).
5. Wilker, E. H. et al. Green space and mortality following ischemic stroke. *Environ. Res.* **133**, 42–48 (2014).
6. Vienneau, D. et al. More than clean air and tranquillity: residential green is independently associated with decreasing mortality. *Environ. Int.* **108**, 176–184 (2017).
7. Ji, J. S. et al. Residential greenness and mortality in oldest-old women and men in China: a longitudinal cohort study. *Lancet Planet. Health* **3**, e17–e25 (2019).
8. Nieuwenhuijsen, M. J. et al. Air pollution, noise, blue space, and green space and premature mortality in Barcelona: a mega cohort. *Int. J. Environ. Res. Public Health* **15**, 2405 (2018).
9. Zijlema, W. L. et al. The longitudinal association between natural outdoor environments and mortality in 9218 older men from Perth, Western Australia. *Environ. Int.* **125**, 430–436 (2019).
10. Orioli, R. et al. Exposure to residential greenness as a predictor of cause-specific mortality and stroke incidence in the Rome longitudinal study. *Environ. Health Perspect.* **127**, 27002 (2019).
11. Rojas-Rueda, D., Nieuwenhuijsen, M. J., Gascon, M., Perez-Leon, D. & Mudu, P. Green spaces and mortality: a systematic review and meta-analysis of cohort studies. *Lancet Planet. Health* **3**, e469–e477 (2019).
12. Yang, B. Y. et al. Greenspace and human health: an umbrella review. *Innovation (Camb.)* **2**, 100164 (2021).
13. GIS Geography. What is NDVI (Normalized Difference Vegetation Index)? https://gisgeography.com/ndvi-normalized-difference-vegetation-index/ (Accessed: 14 October 2024).
14. Nieuwenhuijsen, M. J. Urban and transport planning, environmental exposures and health—new concepts, methods and tools to improve health in cities. *Environ. Health* **15**, 38 (2016).
15. Kondo, M. C., Fluehr, J. M., McKeon, T. & Branas, C. C. Urban green space and its impact on human health. *Int. J. Environ. Res. Public Health* **15**, e445 (2018).
16. Derkzen, M., van Teeffelen, A. J. A. & Verburg, P. Quantifying urban ecosystem services based on high-resolution data of urban green space: an assessment for Rotterdam, the Netherlands. *J. Appl. Ecol.* **52**, 1020–1032 (2015).
17. Nowak, D. J., Crane, D. E. & Stevens, J. C. Air pollution removal by urban trees and shrubs in the United States. *Urban For. Urban Green.* **4**, 115–123 (2006).
18. Litschke, T. & Kuttler, W. On the reduction of urban particle concentration by vegetation—a review. *Meteorol. Z.* **17**, 229–240 (2008).
19. van den Berg, M. et al. Health benefits of green spaces in the living environment: a systematic review of epidemiological studies. *Urban For. Urban Green.* **14**, 806–816 (2015).
20. Konijnendijk, C. Annerstedt, M., Busse Nielsen, A., & Maruthaveeran, S. Benefits of urban parks: a systematic review. *A report for IPFRA* (2013). https://worldurbanparks.org/images/Newsletters/IfpraBenefitsOfUrbanParks.pdf (Accessed: 23 February 2024).
21. de Vries, S., van Dillen, S. M., Groenewegen, P. P. & Spreeuwenberg, P. Streetscape greenery and health: stress, social cohesion and physical activity as mediators. *Soc. Sci. Med.* **94**, 26–33 (2013).
22. Egorov, A. I. et al. Vegetated land cover near residence is associated with reduced allostatic load and improved biomarkers of neuroendocrine, metabolic and immune functions. *Environ. Res.* **158**, 508–521 (2017).
23. Li, Q. et al. Visiting a forest, but not a city, increases human natural killer activity and expression of anti-cancer proteins. *Int. J. Immunopathol. Pharmacol.* **21**, 117–127 (2008).
24. Li, Q. et al. A forest bathing trip increases human natural killer activity and expression of anti-cancer proteins in female subjects. *J. Biol. Regul. Homeost. Agents* **22**, 45–55 (2008).
25. Rook, G. A. Regulation of the immune system by biodiversity from the natural environment: an ecosystem service essential to health. *Proc. Natl Acad. Sci. USA* **110**, 18360–18367 (2013).
26. Konijnendijk, C. C. Evidence-based guidelines for greener, healthier, more resilient neighbourhoods: Introducing the 3-30-300 rule. *J. Res. (Harbin)* **34**, 821–830 (2023).
27. Brochu, P., Jimenez, M. P., James, P., Kinney, P. L. & Lane, K. Benefits of increasing greenness on all-cause mortality in the largest metropolitan areas of the United States within the past two decades. *Front. Public Health* **10**, 841936 (2022).
28. Barboza, E. P. et al. Green space and mortality in European cities: a health impact assessment study. *Lancet Planet. Health* **5**, e718–e730 (2021).
29. Rothman, K. J., Greenland, S. & Lash, T. L. *Modern Epidemiology*. 3rd ed. (Lippincott Williams & Wilkins, 2008).
30. Rothman, K. J. *Epidemiology: An Introduction*. 2nd edn (Oxford University Press, 2012).
31. Porta, M. *A Dictionary of Epidemiology*. 6th edn. (Oxford University Press, 2014).
32. Pearce, N. *A Short Introduction To Epidemiology*. 2nd edn (Centre for Public Health Research, 2005).
33. van den Brenk, I. The use of Health Impact Assessment tools in European Cities. A guide to support policy towards cleaner air and improvement of citizens' health (2018). https://ec.europa.eu/futurium/en/system/files/ged/4.the_use_of_health_impact_assessment_tools_in_european_cities.pdf (Accessed: 19 February 2024).
34. European Topic Centre on Air Pollution and Climate Change Mitigation. Quantifying the health impacts of ambient air pollution: methodology and input data. *ETC/ACM Technical Paper 2016/5* (2017). https://www.eionet.europa.eu/etcs/etc-atni/products/etc-atni-reports/etcacm_tp_2016_5_aq_hia_methodology (Accessed: 19 February 2024).
35. European Topic Centre on Air Pollution, Transport, Noise and Industrial Pollution. Health risk assessment of air pollution in Europe. Methodology description and 2017 results. *Eionet Report - ETC/ATNI 2019/13* (2020). https://www.eionet.europa.eu/etcs/etc-atni/products/etc-atni-reports/etc-atni-report-13-2019-health-risk-assessment-of-air-pollution-in-europe-methodology-description-and-2017-results (Accessed: 19 February 2024).
36. European Topic Centre on Air Pollution, Transport, Noise and Industrial Pollution. Health risk assessments of air pollution. Estimations of the 2019 HRA, benefit analysis of reaching specific air quality standards and more. *Eionet Report - ETC/ATNI 2021/10* (2021). https://www.eionet.europa.eu/etcs/etc-atni/products/etc-atni-reports/etc-atni-report-10-2021-health-risk-assessments-of-air-pollution-estimations-of-the-2019-hra-benefit-analysis-of-reaching-specific-air-quality-standards-and-more (Accessed: 19 February 2024).

37. National Institute for Environmental Protection and Research. Linee guida per la valutazione integrata di impatto ambientale e sanitario (VIIAS) nelle procedure di autorizzazione ambientale (VAS, VIA, AIA). *Manuali e linee guida 133/2016* (2016). https://www.isprambiente.gov.it/it/pubblicazioni/pubblicazioni-del-sistema-agenziale/resolveuid/0b29a7b368424050af0cc5a1fc770f56 (Accessed: 09 October 2024).
38. National Institute of Health. Linee guida per la valutazione di impatto sanitario (DL.vo 104/2017). *Rapporti ISTISAN 19/9* (2019). https://www.iss.it/documents/20126/45616/19_9_web.pdf/4bebb80b-6290-82b8-59d6-0f851ae303cf?t=1581099461900 (Accessed: 09 October 2024).
39. Bauleo, L., Fabri, A., De Santis, M., Soggiu, M. E. & Ancona, C. SENTIERI Project: air pollution and health impact of population living in industrial areas in Italy. *Epidemiol. Prev.* **47**, 338–353 (2023).
40. Galise, I. et al. The Integrated Environmental Health Impact of emissions from a steel plant in Taranto and from a power plant in Brindisi, (Apulia Region, Southern Italy). *Epidemiol. Prev.* **43**, 329–337 (2019).
41. European Environment Agency. Health impacts of air pollution in Europe, 2022. https://www.eea.europa.eu/publications/air-quality-in-europe-2022/health-impacts-of-air-pollution (Accessed: 19 February 2024).
42. Khomenko, S. et al. Premature mortality due to air pollution in European cities: a health impact assessment. *Lancet Planet. Health* **5**, e121–e134 (2021).
43. Barboza, E. P. et al. Environmental health impacts and inequalities in green space and air pollution in six medium-sized European cities. *Environ. Res.* **237**, 116891 (2023).
44. Wolf, K. L. et al. Urban trees and human health: a scoping review. *Int. J. Environ. Res. Public Health* **17**, 4371 (2020).
45. Salmond, J. A. et al. Health and climate related ecosystem services provided by street trees in the urban environment. *Environ. Health* **15**, 36 (2016).
46. Turner-Skoff, J. B. & Cavender, N. The benefits of trees for livable and sustainable communities. *Plants People Planet* **1**, 323–335 (2019).
47. Willis, K. J. & Petrokofsky, G. The natural capital of city trees. *Science* **356**, 374–376 (2017).
48. Kardan, O. et al. Neighborhood greenspace and health in a large urban center. *Sci. Rep.* **5**, 11610 (2015).
49. Beyer, K. M. M. et al. Exposure to neighborhood green space and mental health: evidence from the survey of the health of Wisconsin. *Int. J. Environ. Res. Public Health* **11**, 3453–3472 (2014).
50. Taylor, M. S., Wheeler, B. W., White, M. P., Economou, T. & Osborne, N. J. Research note: urban street tree density and antidepressant prescription rates — a cross-sectional study in London, UK. *Landsc. Urban Plan.* **136**, 174–179 (2015).
51. Donovan, G. H. et al. The relationship between trees and human health: evidence from the spread of the emerald ash borer. *Am. J. Prev. Med.* **44**, 139–145 (2013).
52. Ulmer, J. M. et al. Multiple health benefits of urban tree canopy: the mounting evidence for a green prescription. *Health Place* **42**, 54–62 (2016).
53. Astell-Burt, T. & Feng, X. Urban green space, tree canopy and prevention of cardiometabolic diseases: a multilevel longitudinal study of 46 786 Australians. *Int. J. Epidemiol.* **49**, 926–933 (2020).
54. Schwaab, J. et al. The role of urban trees in reducing land surface temperatures in European cities. *Nat. Commun.* **12**, 6763 (2021).
55. Picot, X. Thermal comfort in urban spaces: impact of vegetation growth - Case study: piazza della Scienza, Milan, Italy. *Energy Build.* **36**, 329–334 (2004).
56. Shashua-Bar, L. & Hoffman, M. E. Vegetation as a climatic component in the design of an urban street - An empirical model for predicting the cooling effect of urban green areas with trees. *Energy Build.* **31**, 221–235 (2000).
57. Wilmers, F. Effects of vegetation on urban climate and buildings. *Energy Build.* **15**, 507–514 (1990–1991).
58. Bressler, R. D. The mortality cost of carbon. *Nat. Commun.* **12**, 4467 (2021).
59. Giannico, O. V. et al. The mortality cost of carbon dioxide emissions from a steel plant in Southern Italy: a climate change health impact assessment. *Epidemiol. Prev.* **47**, 273–280 (2023).
60. Bowler, D. E., Buyung-Ali, L., Knight, T. M. & Pullin, A. S. Urban greening to cool towns and cities: a systematic review of the empirical evidence. *Landsc. Urban Plan.* **97**, 147–155 (2010).
61. Giles-Corti, B. et al. Increasing walking: how important is distance to, attractiveness, and size of public open space? *Am. J. Prev. Med.* **28**, 169–176 (2005).
62. Hillsdon, M., Panter, J., Foster, C. & Jones, A. The relationship between access and quality of urban green space with population physical activity. *Public Health* **120**, 1127–1132 (2006).
63. McCormack, G. R., Rock, M., Toohey, A. M. & Hignell, D. Characteristics of urban parks associated with park use and physical activity: a review of qualitative research. *Health Place* **16**, 712–726 (2010).
64. Sugiyama, T. et al. Initiating and maintaining recreational walking: a longitudinal study on the influence of neighborhood green space. *Prev. Med.* **57**, 178–182 (2013).
65. Sugiyama, T., Francis, J., Middleton, N. J., Owen, N. & Giles-Corti, B. Associations between recreational walking and attractiveness, size, and proximity of neighborhood open spaces. *Am. J. Public Health* **100**, 1752–1757 (2010).
66. Van Dillen, S. M., De Vries, S., Groenewegen, P. P. & Spreeuwenberg, P. Greenspace in urban neighbourhoods and residents' health: adding quality to quantity. *J. Epidemiol. Community Health* **66**, e8 (2012).
67. Pope, D. et al. Quality of and access to green space in relation to psychological distress: results from a population-based cross-sectional study as part of the EURO-URHIS 2 project. *Eur. J. Public Health* **28**, 35–38 (2015).
68. Francis, J., Wood, L. J., Knuiman, M. & Giles-Corti, B. Quality or quantity? Exploring the relationship between Public Open Space attributes and mental health in Perth, Western Australia. *Soc. Sci. Med.* **74**, 1570–1577 (2012).
69. Grahn, P. & Stigsdotter, U. K. The relation between perceived sensory dimensions of urban green space and stress restoration. *Landsc. Urban Plan.* **94**, 264–275 (2010).
70. Annerstedt, M. et al. Green qualities in the neighbourhood and mental health – results from a longitudinal cohort study in Southern Sweden. *BMC Public Health* **12**, 337 (2012).
71. Van den Bosch, M. A., Östergren, P. O., Grahn, P., Skärbäck, E. & Währborg, P. Moving to serene nature may prevent poor mental health – results from a Swedish longitudinal cohort study. *Int. J. Environ. Res. Public Health* **12**, 7974–7989 (2015).
72. Kuo, F. E. & Sullivan, W. C. Aggression and violence in the inner city: effects of environment via mental fatigue. *Environ. Behav.* **33**, 543–571 (2001).
73. Kuo, F. E. Coping with poverty: impacts of environment and attention in the inner city. *Environ. Behav.* **33**, 5–34 (2001).
74. Kuo, F. E., Bacaicoa, M. & Sullivan, W. C. Transforming inner-city landscapes: trees, sense of safety, and preference. *Environ. Behav.* **30**, 28–59 (1998).
75. Bauwelinck, M. et al. Residing in urban areas with higher green space is associated with lower mortality risk: a census-based cohort study with ten years of follow-up. *Environ. Int.* **148**, 106365 (2021).
76. Rodriguez-Loureiro, L. et al. Long-term exposure to residential green spaces and site-specific cancer mortality in urban Belgium: a 13-year follow-up cohort study. *Environ. Int.* **170**, 107571 (2022).

77. Wang, D. et al. Neighbouring green space and mortality in community-dwelling elderly Hong Kong Chinese: a cohort study. *BMJ Open* **7**, e015794 (2017).
78. European Environment Agency. Harm to human health from air pollution in Europe: burden of disease 2023. https://www.eea.europa.eu/publications/harm-to-human-health-from-air-pollution/ (Accessed: 26 April 2024).
79. World Health Organization. Health risk assessment of air pollution: general principles (2016). https://www.who.int/publications/i/item/9789289051316 (Accessed: 26 April 2024).
80. World Health Organization. Health impact assessment. https://www.who.int/health-topics/health-impact-assessment#tab=tab_1 (Accessed: 26 April 2024).
81. Dora, C. *Health Impact Assessment: Past Achievement, Current Understanding, and Future Progress* (ed. Kemm, J.) (Oxford University Press, 2013).
82. World Health Organization. Health impact assessment of steel plant activities in Taranto, Italy (2023). https://www.who.int/europe/publications/i/item/9789289058360 (Accessed: 27 April 2024).
83. International Association for Health Impacts Assessment. Health Impact Assessment. https://www.iaia.org/wiki-details.php?ID=14 (Accessed: 27 April 2024).
84. Centers for Disease Control and Prevention. Health Impact Assessment Resources. https://www.cdc.gov/environmental-health-tracking/php/communications-resources/hia-resources.html (Accessed: 15 October 2024).
85. World Health Organization. AirQ+: software tool for health risk assessment of air pollution. https://www.who.int/tools/airq (Accessed: 27 April 2024).
86. World Health Organization. Health risks of air pollution in Europe – HRAPIE Project. Recommendations for concentration–response functions for cost–benefit analysis of particulate matter, ozone and nitrogen dioxide (2013). https://iris.who.int/handle/10665/153692 (Accessed: 27 April 2024).
87. National Institute of Statistics. Boundaries of administrative units for statistical purposes on 01/01/2023. Administrative boundaries 2022. Non-generalized version (more detailed). https://www.istat.it/it/archivio/222527 (Accessed: 13 June 2023).
88. National Institute of Statistics. Codes of administrative units on 30/06/2023. https://www.istat.it/storage/codici-unita-amministrative/Elenco-comuni-italiani.xls (Accessed: 19 August 2023).
89. National Institute of Statistics. Demo. Demography in numbers. Resident population by sex, age, and marital status as on 01/01/2023. Download Area. Municipalities. https://demo.istat.it/app/?i=POS&l=it (Accessed: 19 August 2023).
90. Global Human Settlement Layer. GHS population grid (R2023). Product: GHS-POP, epoch: 2020, resolution: 100m, coordinate system: Mollweide. https://ghsl.jrc.ec.europa.eu/download.php?ds=pop (Accessed: 18 June 2023).
91. Carioli, A., Schiavina, M., Freire, S. & MacManus, K. GHS-POP R2023A - GHS population grid multitemporal (1975-2030). *European Commission, Joint Research Centre (JRC)*. https://doi.org/10.2905/2FF68A52-5B5B-4A22-8F40-C41DA8332CFE.
92. Carneiro Freire, S., MacManus, K., Pesaresi, M., Doxsey-Whitfield, E., & Mills, J. Development of new open and free multi-temporal global population grids at 250 m resolution. *Geospatial Data in a Changing World; Association of Geographic Information Laboratories in Europe (AGILE) (Organiser)*. AGILE. JRC100523 (2016).
93. European Commission, Joint Research Centre (JRC). GHSL Data Package 2023. *Publications Office of the European Union* (2023). https://doi.org/10.2760/098587.
94. National Institute of Statistics.Dataset with daily deaths in each individual municipality of residence by sex and five-year age classes | 1 January 2011 – 31 October 2023. https://www.istat.it/storage/dati_mortalita/Decessi-comunali-giornalieri-4-13122023.zip (Accessed: 13 January 2024).
95. National Institute of Statistics. Demo. Demography in numbers. Resident population mortality tables. Download Area. Complete provincial data, year 2022. https://demo.istat.it/app/?i=TVM&l=it (Accessed: 13 January 2024).
96. European Space Agency. Copernicus. Sentinel-2. https://www.esa.int/Applications/Observing_the_Earth/Copernicus/Sentinel-2/Satellite_constellation (Accessed: 15 October 2024).
97. Yu, W. et al. Global estimates of daily ambient fine particulate matter concentrations and unequal spatiotemporal distribution of population exposure: a machine learning modelling study. *Lancet Planet. Health* **7**, e209–e218 (2023).
98. European Space Agency. ESA WorldCover 2021. Global land cover product at 10 m resolution for 2021 based on Sentinel-1 and 2 data. https://worldcover2021.esa.int/ (Accessed: 5 October 2023).
99. Wood, S. Package 'mgcv'. *R-manual*. https://stat.ethz.ch/R-manual/R-devel/library/mgcv/html (Accessed: 12 October 2024).

Acknowledgements

We are grateful for the availability of data from the European Union's Copernicus programme, the European Space Agency's WorldCover project, the European Commission's Global Human Settlement Layer project, and the Italian National Institute of Statistics. This work was partly developed within the MISTRAL project (ID: 101095119) in the Horizon Europe programme of the European Union. R.S. and A.M. received funding for the publication of this article (article processing charge) from the CALLIOPE (House of Innovation for One Health) project (ID: E53C22002800001) through the Development and Cohesion Fund of the Ministry of Enterprises and Made in Italy. We are grateful for comments from and discussions with Simona Baldacci and Letizia Lorusso. The opinions expressed in this article are our own and do not necessarily reflect the views of the European Union, the Italian ministries and the governments they represent, or the institutions to which the authors belong.

Author contributions

Conceptualisation, data curation, formal analysis, investigation, methodology, project administration, resources, software, supervision, visualisation, and writing - original draft: O.V.G.; funding acquisition: R.S. and A.M.; validation, and writing - review and editing: O.V.G., R.S., L.B., F.A., F.P., S.M., and A.M.

Competing interests

The authors declare no competing interests.

Additional information

Supplementary information The online version contains supplementary material available at https://doi.org/10.1038/s41467-024-54388-7.

Correspondence and requests for materials should be addressed to Orazio Valerio Giannico.

Peer review information *Nature Communications* thanks John Ji, and the other, anonymous, reviewer(s) for their contribution to the peer review of this work. A peer review file is available.

https://doi.org/10.1038/s41467-024-54388-7